SCIENTIFIC REPORTS

OPEN

Intersubband Transition in GaN/InGaN Multiple Quantum Wells

G. Chen[1], X.Q. Wang[1,2], X. Rong[1], P. Wang[1], F.J. Xu[1], N. Tang[1], Z.X. Qin[1], Y.H. Chen[3] & B. Shen[1,2]

Received: 25 February 2015
Accepted: 26 May 2015
Published: 19 June 2015

Utilizing the growth temperature controlled epitaxy, high quality GaN/$In_{0.15}Ga_{0.85}N$ multiple quantum wells designed for intersubband transition (ISBT) as novel candidates in III-nitride infrared device applications have been experimentally realized for the first time. Photo-absorption originated from the ISBT has been successfully observed at infrared regime covering the 3–5 μm atmosphere window, where the central absorption wavelength is modulated by adjusting the quantum well width. With increasing the quantum well thickness, the ISBT center wave length blue shifts at thickness less than 2.8 nm and then redshifts with further increase of the well thickness. The non-monotonic trend is most likely due to the polarization induced asymmetric shape of the quantum wells.

Since the pioneering discovery of intersubband transition (ISBT) in quantum structures, great concern has been aroused in this area, motivated by the tremendous prospect on infrared optoelectronics, such as quantum well infrared photodetectors (QWIPs), quantum cascade infrared photodetectors (QCIPs), quantum cascade lasers (QCLs), and electro-optic modulators[1–7]. Compared with traditional materials such as Si- or GaAs- based semiconductors, III-nitrides reap the benefit from their unique nature of large conduction band (CB) offset, ultra-short electron relaxation time and large LO-phonon energy[8,9]. Up to date, most efforts with this respect have been devoted to AlGaN/GaN multiple quantum wells (MQWs) towards the detection of 1.3 and 1.55 μm optical communication wavelengths as well as in the terahertz range[10–14]. However, due to the alloy disorder and defects scattering in the AlGaN barriers, it seems hard to acquire high-gain photoconductive response in the AlGaN/GaN MQWs. In addition, the lack of high electron mobility prevents such structures from achieving effective vertical transport across the MQWs. Those facts seriously limit the device performance and restrict the development of GaN-based ISBT detectors.

One of the possible solutions is to use GaN/InGaN MQWs instead. In this case, both of the alloy disorder and defects scattering in the barrier could be significantly reduced since the barrier is no longer AlGaN but GaN which exhibits much larger electron mobility[15]. Furthermore, the growth of GaN/InGaN MQW shave an advantage of easily avoiding cracks since the GaN/InGaN MQWs exhibit compressive strain[16]. However, it remains challenging in the preparation of InGaN upon how to precisely control the In fraction as well as the interface sharpness during the growth. And thus, only theoretical prediction of ISBT energy in GaN/InGaN MQWs have been reported so far[8].

In this article, we will report an experimental observation of the inter-subband transition from c-plane GaN/$In_{0.15}Ga_{0.85}N$ MQWs. Utilizing the growth temperature controlled epitaxy (GTCE) method in molecular beam epitaxy (MBE), high-quality GaN/$In_{0.15}Ga_{0.85}N$ MQWs, which are nearly free of elemental inter-diffusion and phase separation, were successfully grown. The ISBT photo-absorption at infrared regime covering 3–5 μm atmosphere window was successfully achieved. With increasing the thickness of the quantum wells (T_w), the central ISBT wavelength was found to show blue-shift in the MQWs at thickness no more than 2.8 nm and the red-shift with further increase of the well thickness.

[1]State Key Laboratory of Artificial Microstructure and Mesoscopic Physics, School of Physics, Peking University, Beijing 100871, China. [2]Collaborative Innovation Center of Quantum Matter, Beijing, China. [3]Laboratory of Semiconductor Material Science, Institute of Semiconductors, CAS, Beijing 100083, China. Correspondence and requests for materials should be addressed to X.Q.W. (email: wangshi@pku.edu.cn) or B.S. (email: bshen@pku.edu.cn)

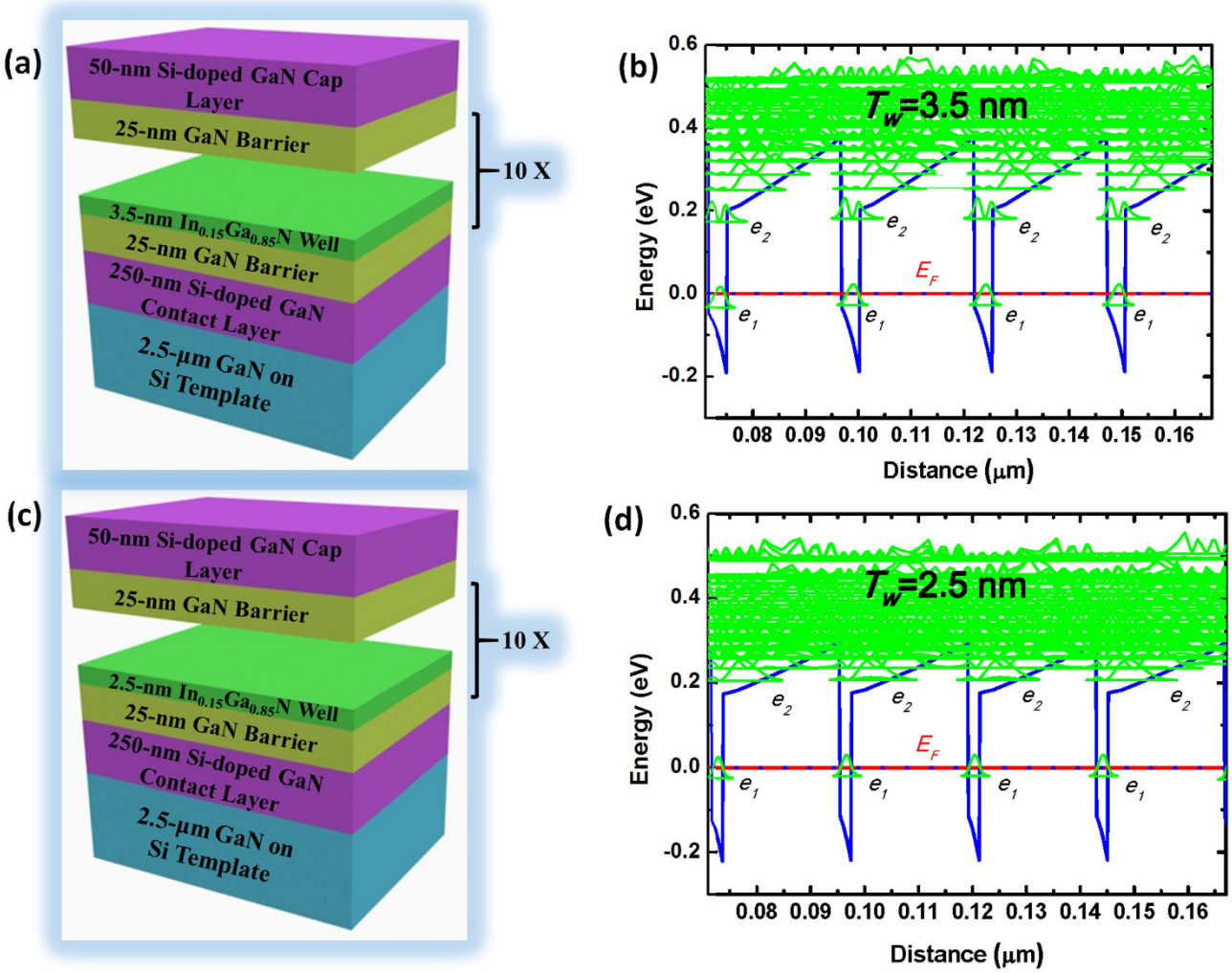

Figure 1. (**a**) Schematic image of structure and (**b**) conduction band profile of GaN/$In_{0.15}Ga_{0.85}N$ (25 nm/3.5 nm) MQWs. (**c**) Schematic image of structure and (**d**) conduction band profile of GaN/$In_{0.15}Ga_{0.85}N$ (25 nm/2.5 nm) MQWs.

Results

We designed the structure of MQWs by self-consistently solving the Schrödinger and Poisson equations. The sample structures are shown in Fig. 1(a),(c), and the corresponding band profiles are shown in Fig. 1(b),(d), respectively. It is shown that the GaN barrier thickness (T_b) is designed as 25 nm and the In composition is optimized to be 15% in InGaN wells for both types of quantum structure. It should be noted that the III-nitride materials exhibit strong internal electric field along c-direction[17–19]. That is referred as an intrinsic property of III-nitrides because of the asymmetric lattice structure. A c-plane GaN/InGaN MQW is asymmetric with a deep quantum well and a relatively wide triangular open mouth due to the polarization induced internal electric field[20]. Thus, the subbands in GaN-based MQWs structure can be divided into two types. One locates inside the well-confined quantum well and the other locates at the open mouth. In Fig. 1(a),(b), the $In_{0.15}Ga_{0.85}N$ quantum well thickness (T_w) was set at 3.5 nm to make the first two subbands confined in the quantum well. In contrast, in Fig. 1(c),(d), T_w was reduced to 2.5 nm to lift all the excited subbands to the open mouth of the quantum well. The latter structure is designed to allow a broad detection range from 200 meV (6.2 μm) to 550 meV (2.25 μm), which covers the range of the 3–5 μm atmosphere window. In both structures, the wells were heavily doped by Si to keep the ground subband below the Fermi level.

Samples were grown by plasma-assisted molecular beam epitaxy. A 2.5-μm-thick GaN layer grown on (111)Si substrate by metal-organic vapor phase epitaxy (MOVPE) was used as template. The (111)Si other than sapphire was used as substrate here is to avoid infrared absorption of the latter one. As shown in Fig. 1(a),(c), the growth started from a 250-nm-thick Si-doped n-type GaN layer, followed by a 25-nm-thick GaN barrier. Then 10 periods of GaN/$In_{0.15}Ga_{0.85}N$ quantum wells were grown setting the barrier thickness of 25 nm. Finally, a 50-nm-thick n-type GaN cap layer was deposited. After

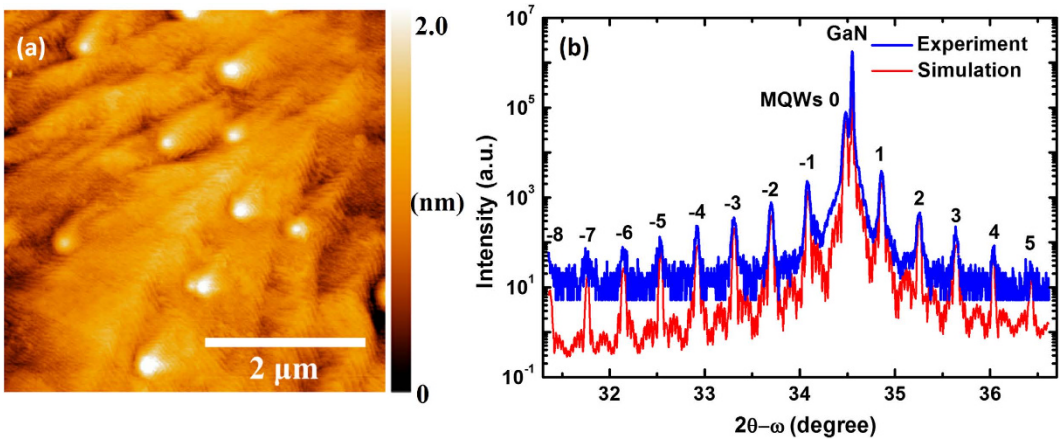

Figure 2. (**a**) Typical AFM image of surface morphology of the grown sample. (**b**) Experimental curve of HR-XRD (0002) 2θ-ω scans for the sample with T_w of 2.5 nm (blue line) and the corresponding simulated curve (red line).

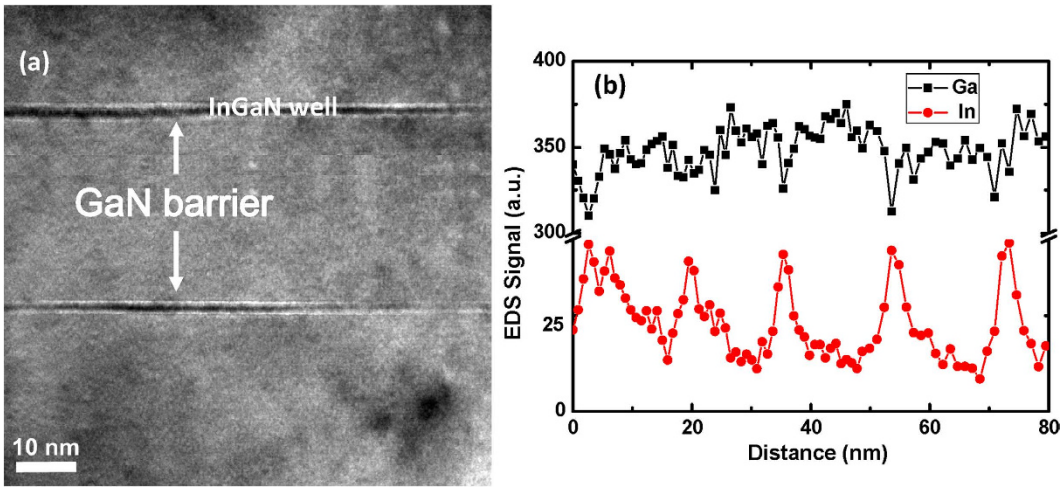

Figure 3. (**a**) Cross-sectional HR-TEM images of GaN/$In_{0.15}Ga_{0.85}N$ MQWs. (**b**) Signal intensity of Ga (black) and In (red) atoms obtained by EDS. The distance is along the growth condition. The periodical distribution of In atom signal is clearly shown.

optimization for the growth parameters, four samples with $In_{0.15}Ga_{0.85}N$ well thicknesses of 2.5, 3, 3.5 and 4 nm were grown for comparison. For all the samples, Si was used as the n-type dopant in the InGaN quantum wells and the residual electron density was about $1 \times 10^{19}\,cm^{-3}$.

As mentioned above, in order to grow high quality InGaN layers, the growth temperature controlled epitaxy is used here[21], where the InGaN layer is grown at its maximum temperature of 620 °C at metal-rich condition, which leads to a flat surface and is helpful for improving the interface sharpness. Figure 2(a) shows the typical surface morphologies of the grown samples, which are free of cracks because the GaN/InGaN MQWs exhibit compressive strain when growing on the GaN:Si templates. The morphology is almost the same as that of homo-epitaxial GaN grown by MBE on MOVPE-grown GaN template. There are some spirals which are most likely due to the screw-component threading dislocations[22]. Except that, step-flow feature is clearly observed and the surface roughness (root mean square value) in a scanned area of $3 \times 3\,\mu m^2$ is less than 0.5 nm. This atomically flat surface coincides with the streaky pattern in the reflection high energy electron diffraction (RHEED) measurement. Figure 2(b) illustrates the high resolution x-ray diffraction (HR-XRD) 2θ-ω scans of the (0002) symmetric plane of the sample with T_w of 2.5 nm. The clearly visible satellite peaks from −8 to +5 orders indicate sharp interfaces between wells and barriers, and excellent periodicity of the MQWs. Estimated barrier and well thicknesses by simulation to the experimental XRD spectra are 23 and 2.3 nm, respectively, with the In composition in the InGaN quantum well of ~0.15, which coincide well with our theoretically designed values.

The interface sharpness of the MQWs is further revealed by high resolution transmission electron microscopy (HR-TEM) image shown in Fig. 3(a). Both the GaN barriers and $In_{0.15}Ga_{0.85}N$ wells are

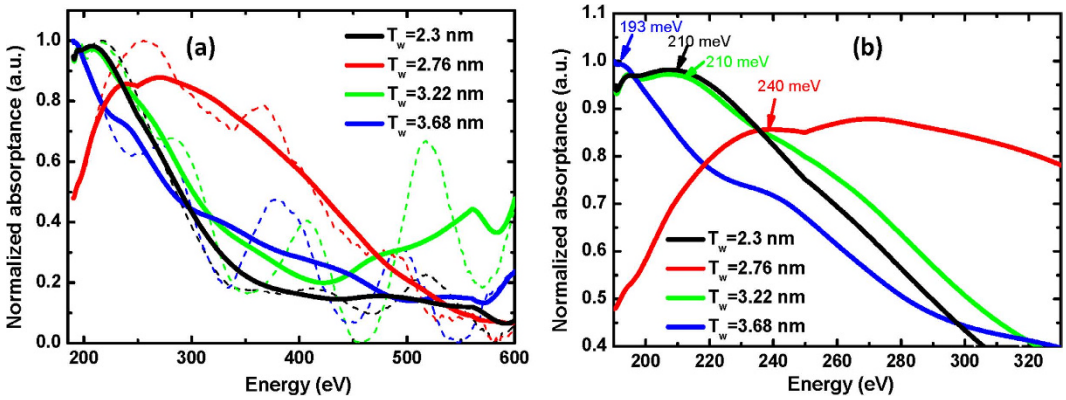

Figure 4. (**a**) Normalized absorption spectra (in dashed lines) and their corresponding fittings (in solid lines) of the GaN/$In_{0.15}Ga_{0.85}N$ MQWs with different well thicknesses. (**b**) The zoomed in absorption spectra without interferenceof the GaN/$In_{0.15}Ga_{0.85}N$ MQWs with different well thicknesses. The absorption peaks due to ISBT from e_1 to $e_2$are marked.

uniform and the interfaces between them are edgily sharp. The composition uniformity of the alloy in the MQWs was investigated by space-resolved scanning of Ga and In atoms using energy dispersive spectrometry (EDS) measurement and their results are shown in Fig. 3(b). It is obvious that the scanned signal is of excellent periodicity and uniformity, being an evidence that the inter-diffusion and phase separation is effectively prevented by controlling the growth condition.

Figure 4 shows photoabsorption spectra measured by Fourier transform infrared spectrometer (FTIR). The 45-degree cut and polished sample waveguides were placed between the grid line polarizer and the detector. P-polarized light was selected as the signal while s-polarized one was set as background according to the optical transition selection rules[23]. The normalized intersubband absorption spectra are shown by dashed lines in Fig. 4(a), where periodic interference peaks caused by difference in refractive index between the epilayer and substrate are observed[24]. The fitted curves for the absorption spectra are also displayed in the figure. The ISBT-induced absorption peaks are visible in the range from 190 to 600 meV, in good agreement with the theoretical estimation. Figure 4(b) shows the zoomed in spectra which show the tenability of the ISBT-induced absorption peaks by adjusting the quantum well thickness. The peak positions of the absorption between the first two subbands (E_{12}) can be estimated by Gaussian fits, which are 210, 240, 210 and 193 meV for T_w = 2.3, 2.8, 3.2, 3.7 nm (these thicknesses are estimated from the best fit to the XRD results), respectively. With increasing T_w, the ISBT-induced absorption peak shows blueshift at T_w = 2.3 and 2.8 nm but redshift for the samples at T_w = 3.2 and 3.7 nm.

Discussion

To figure out the reason why the two different structures show opposite tendency with increasing well thickness, theoretical simulation was performed. Photoabsorption oscillation strength in ISBT is known to depend on the wavefunction overlap of electrons in the ground state (e_1) and the upper subbands. The component in the photo-absorption spectra aroused by E_{12} excitation plays a dominate role because their oscillation strength is much stronger than others[23]. Figure 5 shows calculated energy level position of the first two subbands (e_1 and e_2) and their interval energy (E_{12}) as a function of the quantum well thickness. The experimental data are also included for comparison. The non-monotonic behavior of E_{12} is shown in the calculated results, which is in accord with the experiment data. It should be noted that this kind of non-monotonic dependence of intersubband interval energy on the quantum well thickness is similar to that of E_{13} but not E_{12} in the GaN/AlN superlattices as reported by P. K. Kandaswamy *et al.*[25]. This non-monotonic behavior of E_{12} in the GaN/InGaN MQWs is attributed to that the e_2 position shifts from the open mouth of the well to the QW with increasing T_w. In detail, when T_w is less than 2.8 nm, e_1 is localized in the well and e_2 locates at open mouth of the well. However, when T_w is larger than 2.8 nm, both e_1 and e_2 are in the wells. In the former case, the energy position of e_1 decreases with increasing T_w since the electron quantum confinement gets weaker while the energy level of e_2 was only slightly lifted with increasing T_w because the effective barrier height is increased[26,27]. Therefore, their interval energy (E_{12}) gets larger. In the latter case, both e_1 and e_2 drop with increasing T_w, but E_{12} becomes smaller since e_2 falls quicker than e_1. Consequently, the photoabsorption peak blueshifts at first and then redshifts with increasing T_w from 2.3 to 3.7 nm. On the other hand, in GaN/AlN Superlattices, the conduction-band offset (CBO) (around 1.8 eV[25]) is large enough for the first two subbands (e_1 and e_2) confined in several-monolayer-thick GaN well while e_3 locates around the open mouth of well. Thus E_{12} shows monotonic redshift and the E_{13} shows non-monotonic behavior with the increasing well thickness, just as reported by P. K. Kandaswamy *et al.*[25].

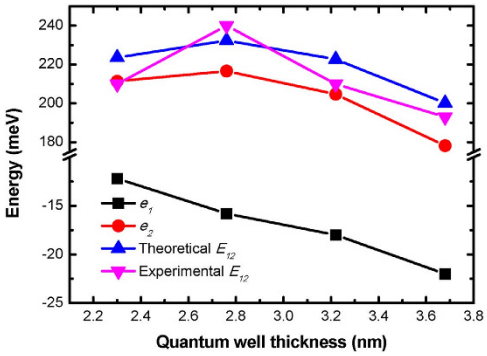

Figure 5. The energy level position of ground subband (e_1, solid black squares), the second subband (e_2, solid red circles), their theoretical interval energy (theoretical E_{12}, solid pink triangles) and experiment interval energy (experimental E_{12}, solid blue triangles) as a function of well thickness.

In summary, high quality GaN/$In_{0.15}Ga_{0.85}N$ MQWs with ultra-sharp interfaces grown by MBE towards ISBT detectors in the atmospheric window have been investigated. The ISBT-induced photoabsorption at infrared region in the GaN/InGaN MQWs was successfully achieved, and the central wavelength can be effectively tuned from 5.2 to 6.4 μm by adjusting the thickness of the quantum wells. The central ISBT wavelength was first red shift and then blue shift in MQWs structure with increasing well thickness, which agrees with the theoretical estimation. The experimental evidence of ISBT in GaN/InGaN MQWs will open a new window for GaN based ISBT devices.

Methods

Fabrication. The samples were grown by plasma-assisted molecular beam epitaxy (SVTA). Atomic nitrogen was provided by an rf-plasma cell with typical nitrogen gas flow rate of 1.2 sccm. Ga, In and Si molecular beams were provided by conventional effusion cells with typical tell temperatures of 1000 °C, 860 °C and 1150 °C, respectively. The typical growth rate for the GaN and InGaN layer is about 1.5 Å/sec. The 2.5-μm-thick GaN layer, which were used as template for the quantum wells epitaxy, were grown on (111)Si substrate by low-pressure metal-organic vapor phase epitaxy (MOVPE) system by using trimethylgallium (TMG) and ammonia (NH_3) as precursors, and H_2/N_2 as the carrier gas. Growth of the quantum wells was in-situ monitored by Reflection High-Energy Electron Diffraction (RHEED), where the streaky pattern was observed continuously, indicating an atomically flat surface.

Numerial simulation. The self-consistent Schrödinger-Poisson equations assumed periodic potential conditions and charge neutrality conditions. In the calculation, the band gap was chosen to be 3.4 eV (0.65 eV) for GaN (InN), and the band gap bowing parameter for InGaN was set as 1.9 eV[21]. The ratio of conduction band offset to the total band offset was set as 65%. The lattice constants, spontaneous polarization and piezoelectric constants of GaN and InN were cited from Ref. 19. The thickness of InGaN quantum wells was carefully determined so that the intersubband transition (ISBT) energy between e_1 and e_2 is able to cover an infrared detection range of 3–5 μm atmosphere window.

Measurements. The surface morphologies of the sample were analyzed by atomic force microscopy (AFM, Bruker Dimension Icon). The crystalline quality of the samples was characterized by high-resolution x-ray diffraction (HR-XRD, Bruker D8) and high-resolution transmission electron microscopy (HR-TEM, Tecnai F30). Residual carrier concentration was investigated by Hall-effect measurement system (ACCENT-HL5500). For infrared measurements, the sample was mechanically polished into 45° waveguides. The photoabsorption spectra were measured by Fourier transform infrared spectrometer (FTIR, Bruker IFS120).

References

1. West, L. C. & Eglash, S. J. First observation of an extremely larg-dipole infrared transition within the conduction band of a GaAs quantum well, *Appl. Phys. Lett.* **46,** 1156 (1985).
2. Smith, J. *et al.* A new infrared detector using electron emission from multiple quantum wells. *J. Vac. Sci. Technol. B* **1,** 376 (1983).
3. Levine, B. Quantum well infrared photodetectors. *J. Appl. Phys.* **74,** R1 (1993).
4. Sirtori, C. *et al.* GaAs/AlGaAs quantum cascade lasers. *Appl. Phys. Lett.* **73,** 3486 (1998).
5. Gendron, L. *et al.* Quantum cascade photodetector. *Appl. Phys. Lett.* **85,** 2824 (2004).
6. Julien, F. H. *et al.* Novel all-optical 10 um waveguide modulator based on intersubband absorption in GaAs/AlGaAs quantum wells. *Appl. Phys. Lett.* **59,** 2645 (1991).
7. Holmstrom, P. Electroabsorption modulator using intersubband transition in GaN-AlGaN-AlN step quantum wells. *IEEE Journal of Quantum Electronics* **42,** 810 (2006).
8. Beeler, M., Trichas, E. & Monroy, E. III-nitride semiconductors for intersubband optoelectronics: A Review, *Semicond. Sci. Technol.* **28,** 074022 (2013).
9. Wu, F. *et al.* Terahertz intersubband transition in GaN/AlGaN step quantum well. *J. Appl. Phys.* **113,** 154505 (2013).

10. Jovanovic, V. *et al.* Designing strain-balanced GaN/AlGaN quantum well stuctures:application to intersubband devices at 1.3 and 1.55 um wavelengths. *J. Appl. Phys.* **93,** 3194 (2003).
11. Kishino, K. *et al.* Intersubband transition in (GaN)m/(AlN)n superlattices in the wavelength ragne from 1.08 to 1.61 um. *Appl. Phys. Lett.* **81,** 1234 (2002).
12. Machhadani, H. *et al.* Terahertz intersubband absorption in GaN/AlGaN step quantum wells. *Appl. Phys. Lett.* **97,** 191101 (2010).
13. Sudradjat, F. F. *et al.* Far-infrared intersubband photodetectors based on double-step III-nitride quantum wells. *Appl. Phys. Lett.* **100,** 241113 (2012).
14. Beeler, M. *et al.* Terahertz absorbing AlGaN/GaN multi-quantum-wells: Demonstration of a robust-4 layer design. *Appl. Phys. Lett.* **103,** 091108 (2013).
15. Ruterana, P., Albrecht, M. & Neugebauer, J. *Nitride semiconductors*. doi: 10.1002/3527607641.indsub, (2003).
16. Jain, S. *et al.* Ion channeling studies on mixed phases formed in metalorganic chemical vapor deposition grown Mg-doped GaN on Al2O3(0001). *J. Appl. Phys*. **87,** 965 (2000).
17. Wu, T. *et al.* Effect of polarization on intersubband tansitions of AlGaN/GaN multi-quantum wells. *Chinese Physics B* **22,** 057302 (2013).
18. Wood, C. & Jena, D. Polarization Effects in Semiconductors: From Ab Initio Theory to Device Applications. e-ISBN 978-0-387-68319-5, (2007).
19. Ambacher, O. *et al.* Two-dimentional electron gases induced by spontaneous and piezoelectric polarization charges in N- and Ga-face AlGaN/GaN heterostructures. *J. Appl. Phys.* **85,** 3222 (1999).
20. Ambacher, O. *et al.* Pyroelectric properties of Al(In)GaN/GaN hetero- and quantum wells. *J. Phys.: Condens. Matter* **14,** 3399 (2002).
21. Liu, S. T. *et al.* Temperature-controlled epitaxy of InGaN alloys and their band gap bowing. *J. Appl. Phys.* **110,** 113514 (2011).
22. Heying, B. *et al.* Control of GaN surface morphologies using plasma-assisted molecular beam epitaxy, *J. Appl. Phys.* **88,** 1855 (2000).
23. Hofstetter, D. *et al.* Photodetectors based on intersubband transistions using III-nitride superlattice structures. *J. Phys.: Condens. Matter* **21,** 174208 (2009).
24. Huang, C. C. *et al.* Intersubband transition at atmospheric window in AlGaN/GaN multiple quantum wells grown on GaN/sapphire templates adopting AlN/GaN superlattices interlayer. *Appl. Phys. Lett.* **98,** 132105 (2011).
25. Kandaswamy, P. K. *et al.* GaN/AlN short-period superlattices for intersubband optoelectronics: A systematic study of their epitaxial growth, design, and performance. *J.Appl. Phys.* **104,** 093501 (2008).
26. Tchernycheva, M. *et al.* Systematic experimental and theoretical investigation of intersubband absorption in GaN/AlN quantum wells. *Phys.Rev. B* **73,** 125347 (2006).
27. Machhadani, H. *et al.* GaN/AlGaN intersubband optoelectronic devices. *New J. Phys.* **11,** 125023 (2009).

Acknowledgments

This work was partly supported by the National Basic Research Program of China (No. 2012CB619300 and 2013CB632800), the National Natural Science Foundation of China (No. 61225019, 61376060 and 61411130214), the National High Technology Research & Development Project of China (No. 2014AA032606) and Beijing Municipal Science and Technology Project (No. Z131100005913001). We also acknowledge Prof. Weikun Ge's critical reading of the manuscript.

Author Contributions

X.Q.W. supervised the project. G.C. and X.Q.W. designed the experiment. G.C., X.Q.W., X.R. and F.J.X. performed the sample growth. G.C., X.R., P.W. and Y.H.C. carried out the measurements of AFM, XRD, TEM and FTIR. X.R. performed the numerical simulations. G.C. and X.Q.W. wrote the manuscript. X.Q.W., F.J.X., N.T., Z.X.Q. and B.S. gave scientific advices. All the authors discussed the results and reviewed the manuscript.

Additional Information

Competing financial interests: The authors declare no competing financial interests.

How to cite this article: Chen, G. *et al.* Intersubband Transition in GaN/InGaN Multiple Quantum Wells. *Sci. Rep.* **5**, 11485; doi: 10.1038/srep11485 (2015).